

## Local structure and order in the semiconductor alloy $\text{Hg}_{0.78}\text{Cd}_{0.22}\text{Te}$ by multinuclear NMR

D. B. Zax

*Baker Laboratory, Department of Chemistry, Cornell University, Ithaca, New York 14853-1301*

D. Zamir

*Solid State Physics Department, Soreq Nuclear Research Center, Yavne 70600, Israel*

S. Vega

*Department of Chemical Physics, Weizmann Institute of Science, Rehovot 76100, Israel*

(Received 25 August 1992)

Multinuclear solid-state nuclear-magnetic-resonance (NMR) experiments have been performed on a single-crystal sample of bulk composition  $\text{Hg}_{0.78}\text{Cd}_{0.22}\text{Te}$ . The NMR spectra of the three distinct lattice species (Hg, Cd, and Te) have been observed and assigned. Some double-resonance Hg-Te and Hg-Cd experiments clarify the assignment of Te resonance to chemical environment. These experimental results confirm our previous assignments of Te shifts to distinct chemical environments. They further suggest that in melt-grown, homogeneously distributed samples, cation distributions differ little from predictions of a statistical model.

### INTRODUCTION

While much of our understanding of alloy systems has been developed using thermodynamic models which ignore the atomistic details, more recent work has rediscovered the influence of local and chemical factors on alloy properties. Boyce and Mikkelsen's extended x-ray-absorption fine-structure (EXAFS) studies of semiconductor alloys<sup>1</sup> clearly showed how, in ternary systems, elements of the binary precursor compounds survived the alloying process. While average bond lengths varied linearly with concentration in accord with Vegard's law, individual bond lengths were shorter and longer than average depending upon whether the binary compounds with the same pairs of atoms were either longer or shorter than those of the alloy. Their observations catalyzed new attempts to study the influence of microscopic bonding patterns on alloy properties. Theoretical formalisms which predict equilibrium properties including atomic distributions are now available for several semiconductor alloys including both III-V (e.g., GaAs with AlAs) and II-VI (e.g., HgTe with CdTe) systems.<sup>2-5</sup> Technological interest in these systems is driven by the ability to use the concentration parameter to tailor electronic properties.

In an earlier study of crystalline samples of  $\text{Hg}_x\text{Cd}_{1-x}\text{Te}$  with varying cation concentration  $x$ , Willig, Sapoval, Leiber, and Verie<sup>6</sup> demonstrated that solid-state  $^{199}\text{Hg}$  nuclear magnetic resonance (NMR) was capable of monitoring changes in bulk composition, and they suggest how the observed spectra might reflect bonding properties in the alloy. Somewhat later,<sup>7-9</sup> we demonstrated that solid-state  $^{125}\text{Te}$  NMR was a technique with sufficient chemical sensitivity to provide information about local structure and ordering. Measurement of the Te NMR spectrum is possible with good sensitivity for all concentrations  $0 \leq x \leq 1$ , and by observing the appear-

ance and disappearance of spectral lines, it was possible to assign specific ranges of line frequencies to the various possible microenvironments  $\text{Te}_q$  (i.e., Te surrounded by  $q$  Hg first-nearest neighbors and  $(4-q)$  Cd first-nearest neighbors). It was suggested<sup>7</sup> that certain of the best-resolved powder spectra were inconsistent with available models of semiconductor alloys in that the populations of microenvironments  $P^q(x)$ , of the different microenvironments appeared to differ substantially from predictions of available theory. While ordering has been found in ternary alloy systems,<sup>2-5</sup> the existence of substantial ordering in high-temperature grown melts was difficult to rationalize.

The surprising nature of these conclusions led us to reexamine the question of the Te chemical shift assignments and our interpretation of the measured line intensities. In addition, we subsequently observed the solid-state  $^{111}\text{Cd}$ ,  $^{113}\text{Cd}$ , and  $^{199}\text{Hg}$  NMR spectra of these same powders, as well as samples subsequently prepared so as to be nonstoichiometric in the cation-to-anion ratios. As the Hg NMR absorption frequency is so sensitive to compositional effects in these alloys,<sup>6</sup> the discovery that many of the Hg spectra consisted of multiple lines seemed to indicate an inhomogeneous distribution of compositional environments. A most important element in theoretical calculations of microstructural distributions in alloys such as  $\text{Hg}_x\text{Cd}_{1-x}\text{Te}$  is the concentration parameter  $x$ . Particularly in  $\text{Hg}_x\text{Cd}_{1-x}\text{Te}$ , where the lattice dimension varies little with composition, it appears that Hg NMR may be superior to x-ray methods in revealing microscopic inhomogeneities. (In contrast, the Cd NMR spectrum appeared relatively insensitive to composition and a relatively poor diagnostic for structural features.) Therefore, it was considered essential that further studies emphasize well-characterized single-crystal samples. This paper presents extended measurements on a single sample with

bulk composition  $\text{Hg}_{0.78}\text{Cd}_{0.22}\text{Te}$  and reports on the implications of these measurements.

### THE SAMPLE

The specific composition  $\text{Hg}_{0.78}\text{Cd}_{0.22}\text{Te}$  has found wide use as an infrared detector. The bulk composition parameter  $x$  in our samples was determined by measuring the alloy energy gap  $E_g$  by infrared absorption and using the calibration curves relating  $E_g$  and  $x$ .<sup>10</sup> As-grown samples have large numbers of free carriers primarily due to Hg vacancies in the lattice. Each vacancy is an acceptor site, and these uncompensated holes result in  $p$ -type as-grown samples. Post growth annealing in Hg removes these vacancies, and the remaining material is typically  $n$ -type due to a much smaller number of residual donor sites.<sup>11</sup> In better quality samples, thermal carriers dominate the room-temperature conductivity.

The sample discussed in this paper was “ $p$ -type as-grown” and derived from a high-temperature melt. A similar sample from the same melt which was subsequently subjected to a Hg annealing treatment was “ $n$  type” and of device quality. Ideally, all experiments would have been executed on the best quality samples available. Nonetheless, all of the experiments described in this paper were performed on an “as-grown” sample so as to minimize the necessary measurement time. One of the most important parameters in determining the minimum required experimental period is the free-carrier concentration because it, in large part, determines the nuclear spin-lattice relaxation time  $T_1$ . It is this latter parameter which determines how rapidly subsequent scans can be accumulated, which is quite important when extensive signal averaging is required. While the NMR spectra for  $p$ - and  $n$ -type samples varied little,  $T_1$  was typically an order of magnitude longer in the annealed (more  $n$ -type) samples. As the series of experiments described in this paper proved to be quite time consuming, this argued rather strongly for executing the most demanding experiments on  $p$ -type samples only. A subsequent publication will report  $T_1$  measurements, and their implications, in a number of samples of similar composition, but differing electrical properties.

### NMR BACKGROUND

Table I reports the nominal resonance frequencies and isotopic abundances for the relevant nuclear spin species in  $\text{Hg}_x\text{Cd}_{1-x}\text{Te}$  in our magnetic field of 4.7 T. Each is spin  $\frac{1}{2}$  and sits in a relatively dilute magnetic matrix with (typically) zero or one magnetic nuclei (by necessity heteronuclear) in the first coordination sphere. Under conditions of high resolution such as can be achieved under magic-angle sample spinning, the binary compounds reveal structure due to both isotropic shifts and, for spin- $\frac{1}{2}$  nuclei immediately next to other spin- $\frac{1}{2}$  nuclei,  $J$  couplings. The isotropic  $J$  couplings measured in the binary compounds are large ( $J_{\text{iso}} \approx 680$  Hz in CdTe,  $J_{\text{iso}} \approx 5000$  Hz in HgTe).<sup>12</sup> The anisotropic contributions are more difficult to estimate, though for first-nearest neighbors, the dipole-dipole coupling is  $\omega_D \approx 200$  Hz and

TABLE I. NMR spectral parameters for spin- $\frac{1}{2}$  nuclei in  $\text{Hg}_x\text{Cd}_{1-x}\text{Te}$  at 4.7 T.

Nucleus	Resonance frequency (MHz)	Natural Abundance
$^{125}\text{Te}$	63.18	6.99%
$^{199}\text{Hg}$	35.65	16.84%
$^{113}\text{Cd}$	44.37	12.26%
$^{111}\text{Cd}$	42.41	12.75%

for second-nearest neighbors,  $\omega_D \approx 50$  Hz. Anisotropic and isotropic contributions to the  $J$  coupling may be comparable in magnitude.

Previous studies of powder samples showed that where  $^{125}\text{Te}$  is the observed nucleus, and at concentrations  $0.1 < x < 0.9$ , magic-angle sample spinning provided little discernible narrowing.<sup>7,9</sup> This suggests local disorder produces a distribution of local environments (although there may be a small and unidentified contribution to Te linewidths from couplings to the quadrupolar nucleus  $^{201}\text{Hg}$ , natural abundance 13.2%). The current work confirms this observation and extends it to the spectra of the Hg and Cd nuclei as well. This suggests that, except in the binary compounds CdTe and HgTe, spectral features in the alloy systems are dominated by single-spin interactions and are therefore sensitive primarily to interactions with the electronic environment, though there is potentially a similar distribution in isotropic  $J$  couplings.

In conducting and semiconducting samples, large line shifts may be expected. The magnetic fields created by delocalized electrons in the conduction band generate Knight shifts which for metals may be as large as a few percent of the Larmor frequency. In semiconductors, where there are substantially fewer polarizable electrons, and particularly where the constituent atomic species have large atomic numbers, chemical shifts are likely to be the largest interaction. The Te NMR frequencies for the binary compounds CdTe and HgTe differ by 200 ppm. Previous work has suggested that  $^{125}\text{Te}$  shifts in a variety of binary compounds differ in a predictable fashion with bond ionicity, and therefore reflect primarily the effect of chemical shift differences.<sup>13</sup>

We expected that this shift dispersion would be sufficient to observe all of the alloy peaks and that the line positions associated with the different microenvironments  $\text{Te}_q$  would line up between those of the two binary compounds, in rough analogy to  $^{29}\text{Si}$  shifts in zeolites.<sup>14,15</sup> Instead, we found that the bandwidth necessary to observe all the Te signal intensities in the alloys (all of whose band gaps and free-carrier concentrations fall between those of the two binary compounds) cover more than 1000 ppm at frequencies which are exclusively higher (lower field) than are found in CdTe, whose  $^{125}\text{Te}$  spectrum we will choose as our reference standard. (CdTe has been reported to appear at  $-2620$  ppm from the more usual Te standard, dilute  $\text{K}_2\text{TeO}_3$  in  $\text{D}_2\text{O}$ .<sup>16</sup>) These large shift differences appear unrelated to differential Knight shifts, as only small shift differences

(ca. 60 ppm, and relatively insensitive to  $q$ ) are observed in the Te NMR spectra of  $n$ - and  $p$ -type samples of similar bulk composition. While similar nonmonotonic progressions of NMR chemical shifts as a function of number and kind of directly bound substituents have been observed in numerous other systems,<sup>17</sup> its source as well as the magnitude of the shifts observed in these compounds remain unexplained.

### SPECTROSCOPY OF Te SITES

In earlier studies on powder samples, we were led to the conclusion that the intensities of the various lines associated with  $\text{Te}_q$  could be simulated only if we assumed substantial deviations from a statistical distribution of the cations. While x-ray measurements might be consistent with a single-phase material, interpretation of the x-ray results is complicated because of the near coincidence of lattice constants for HgTe, CdTe, and their alloys. Furthermore, in samples of similar bulk composition the relative line intensities varied noticeably between the powder and crystalline samples, and between powders of similar nominal composition but independent preparation. Different crystals of the same bulk composition showed much smaller sample-dependent variations.

It was therefore decided to explore further the assignments and compositional effects in the crystalline samples, where standard measurements in addition to  $^{199}\text{Hg}$  NMR could be used to monitor simultaneously the sam-

ple quality. Our goal was to assign frequencies in the moderately resolved  $^{125}\text{Te}$  NMR spectrum to specific microclusters  $\text{Te}_q$ . A series of spin-echo spectra (obtained with a standard  $\pi/2-\tau-\pi-\tau$  pulse sequence) was observed with varying repetition rates  $t_{\text{rep}}$ , ranging from 0.125 to 120 seconds. The interpulse spacing  $\tau$  was short enough (typically less than 100  $\mu\text{s}$ ) so that line intensities were unaffected by differential spin-spin ( $T_2$ ) dephasing times. The data set for  $t_{\text{rep}} = 30$  s was chosen as representative of the "fully relaxed"  $^{125}\text{Te}$  NMR spectrum and fit via a least-squares simplex-based routine to a minimum number of parameters. A reasonable fit required three distinct spectral lines (each assumed to have identical Lorentzian broadening but variable frequency, amplitude, and Gaussian broadening), as is shown in Fig. 1. The relative line frequencies and integrated intensities are shown in Table II. The line frequencies can be assigned (consistent with previous  $x$ -dependent studies<sup>7,9</sup>) in either of two ways, depending upon whether we assign the broad component centered at approximately 420 ppm to  $\text{Te}_4$  or  $\text{Te}_2$ . Either assignment would be consistent with the range of shifts observed for these environments in cation-concentration-dependent studies, though it was generally observed that the  $\text{Te}_4$  species broadened out most rapidly. Either assignment is unsatisfying because the average Hg lattice concentration  $x_{\text{exp}}$ , as observed by the Te nuclei, can be simply calculated, and

$$x_{\text{exp}} = \frac{1}{4} \sum_q q P^q(x).$$

Assigning the broad species at 420 ppm to  $\text{Te}_4$ , we calculate  $x_{\text{exp}} \approx 0.83$ . The other possible assignment (that the narrow species at 419 ppm is  $\text{Te}_4$ ) suggests  $x_{\text{exp}} \approx 0.68$ . Neither is a particularly good reproduction of the experimentally measured bulk concentration parameter  $x = 0.78$ .

It is clear that we require an internally consistent manner for assigning spectral line positions to the varying local environments. Key to the proper assignment of shift frequencies to chemical environment is the existence of the spin- $\frac{1}{2}$  isotope  $^{199}\text{Hg}$  (although in Cd-rich environments, an entirely analogous experiment might be per-

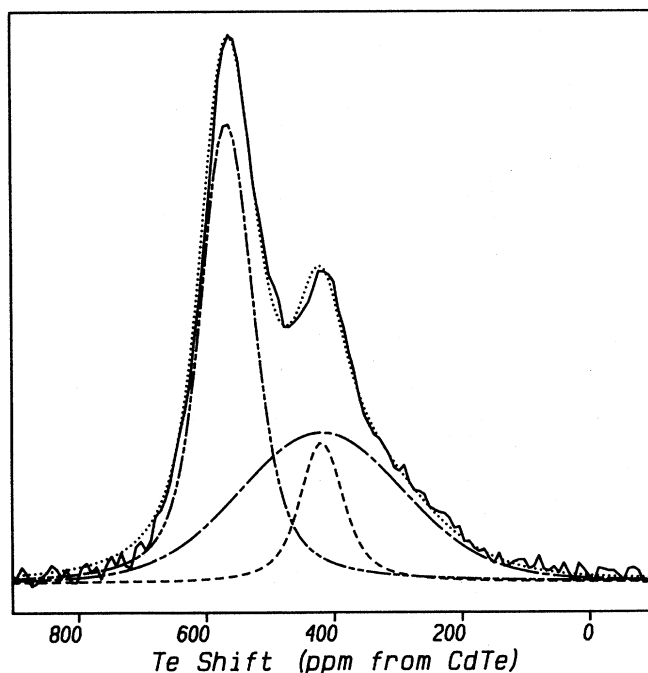


FIG. 1. Experimentally observed spectrum of one  $p$ -type sample of  $\text{Hg}_{0.78}\text{Cd}_{0.22}\text{Te}$ , as described in the text, and least-squares fit to spectrum based on the assumption of three discrete spectral bands. Peak positions, widths, and intensities as described in Table I. Peak 1, -----; peak 2, ———; peak 3, - - -; sum over three subspectra, . . . .

TABLE II. Simulated Te spectra, fit to three lines. Line shapes for the individual lines are produced by a convolution of a Gaussian with width as specified in the Table, and a Lorentzian of width 3.2 kHz. Based on these assignments and intensities, the average Hg lattice occupancy  $x_{\text{exp}}$  is calculated to be either 0.83 or 0.68.

Peak number	1	2	3
Band Center (ppm from CdTe)	564	420	419
Gaussian width (kHz)	3.0	17.4	4.2
Assignment	$\text{Te}_3$	$\text{Te}_4$ or $\text{Te}_2$	$\text{Te}_4$ or $\text{Te}_2$
Integrated intensity	0.47	0.41	0.12

formed using either of the spin- $\frac{1}{2}$  Cd isotopes). We have proposed that the different  $\text{Te}_q$  sites are frequency shifted by the differing environments associated with the  $q$  Hg first-nearest neighbors. For those  $^{125}\text{Te}$  sites with the specific isotope  $^{199}\text{Hg}$  as a neighbor, the additional splittings due to the magnetic interactions between nearby nuclear spins can be used to clarify the issue of the proper correspondence between  $^{125}\text{Te}$  resonance frequency and local environment.

The experiment we have performed (Fig. 2) is a hybrid of the classic Carr-Purcell experiment (with the Meiboom-Gill modification)<sup>18,19</sup> and the spin-echo double-resonance (SEDOR) experiments<sup>20</sup> popularized by Slichter and co-workers.<sup>21-23</sup> After an initial  $\pi/2$  pulse initiates a Te free-induction decay, a string of closely spaced  $\pi$  pulses follow and an echo signal is observed. Ideally, the echo signal refocuses dephasing due both to chemical shift dispersion and heteronuclear couplings to neighboring spin- $\frac{1}{2}$  nuclei ( $^{199}\text{Hg}$ ,  $^{111}\text{Cd}$ , or  $^{113}\text{Cd}$ ). We can selectively refocus only certain heteronuclear couplings by applying  $\pi$  pulses to any of these magnetic nuclei; in our case, the  $^{199}\text{Hg}$  spins. Then the echo decay depends on these couplings as well.

Correlations between the couplings and shift frequencies are achieved by performing the entire experiment in a two-dimensional fashion, i.e., by monitoring the free-induction decay in  $t_2$  (dominated by the shift information) following a period of spin-echo evolution in  $t_1$  (dominated by the selectively refocused heteronuclear dipolar interactions). The experiment is performed as a function

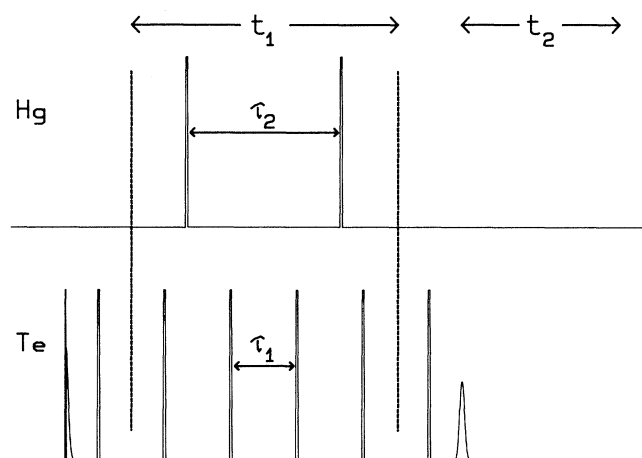


FIG. 2. Two-dimensional NMR pulse sequence for correlation of Te shifts to number of Hg nearest neighbors. The pulse sequence applies a  $\pi/2$  pulse to Te followed by a sequence of phase-shifted  $\pi$  pulses. During  $t_1$ , four  $\pi$  pulses are applied to  $^{125}\text{Te}$  nuclei spaced by a time interval  $\tau_1$  for each pair of  $\pi$  pulses applied to  $^{199}\text{Hg}$  nuclei spaced apart in time by  $\tau_2$ . The scaling factor for the heteronuclear coupling during  $t_1$  is  $(\tau_2/2\tau_1) - 1$ . The experiment is repeated by applying the sequence of four Te and two Hg pulses  $l$  times, for  $l=0$  to 63. For each value of  $l$  the Te echo signal is sampled during the interval  $t_2$ .

of the  $t_1$  evolution period, i.e., the number of  $^{125}\text{Te}$   $\pi$  pulses applied. Double Fourier transformation provides a spectrum of linewidths due to heteronuclear couplings in  $\omega_1$  as a function of the  $^{125}\text{Te}$  spectral frequencies in  $\omega_2$  (see Fig. 3).

We focus temporarily on the spectra observed in  $\omega_1$ , where we have retained the heteronuclear couplings. The width and shape of the observed pattern is a complicated function of the statistical probability of finding  $m$   $^{199}\text{Hg}$  sites among the  $q$  first-nearest Hg neighbors (of whichever isotope), the size of the couplings between Hg and Te, and the distribution of orientations of  $\text{Te}_q$  sites in the applied magnetic field. We attempt no detailed analysis because none is necessary. All we require is an identification of the shifts associated with the different  $\text{Te}_q$  species. Given the reasonable assumption that the magnitude of the  $J$  coupling is similar for all Hg-Te bonds, the widest patterns in  $\omega_1$  correspond to the largest number of  $^{199}\text{Hg}$  nuclei coupled to a single  $^{125}\text{Te}$  nucleus. Because the  $^{199}\text{Hg}$  sites are statistically distributed with respect to all Hg lattice sites, the largest values of  $m$  correspond to the largest values of  $q$  as well, and the crosspeaks uniquely identify the spectral frequencies associated with the  $\text{Te}_q$  microenvironments.

The two-dimensional spectrum is dominated by a large ridge of intensity at  $\omega_1=0$  corresponding to  $\text{Te}_q$  sites with no  $^{199}\text{Hg}$  neighbors [Fig. 3(a)]. This latter can be suppressed by subtracting the signal obtained from a Carr-Purcell sequence executed without Hg pulses [Fig. 3(b)] from that obtained with the Hg pulses. Sites without  $^{199}\text{Hg}$  neighbors evolve identically in either case. The residual signal [Fig. 3(c)] corresponds to only those  $^{125}\text{Te}$  sites with  $^{199}\text{Hg}$  neighbors and moderate-to-large Te-Hg couplings.

Measuring the width is complicated by the problem of limited signal-to-noise ratios. Some improvement in the appearance of the spectrum can be easily achieved in certain simple ways; in particular, it is possible to partially scale the widths of all spectra in  $\omega_1$  uniformly. Applying  $\pi$  pulses to Hg at times exactly coincident with the Te  $\pi$  pulses preserves the entire heteronuclear coupling. We,

TABLE III. Simulated Te spectra, fit to four lines. Line shapes for the individual lines are produced by a convolution of a Gaussian with width as specified in the Table, and a Lorentzian of width 3.2 kHz. Based on these assignments and intensities, the average Hg lattice occupancy is calculated to be 0.77. The statistical probabilities for the microclusters  $\text{Te}_q$  are calculated from  $\binom{4}{q}x^q(1-x)^{(4-q)}$  and  $x=0.78$ .

Peak numbers	1	2	3	4
Band center (ppm from CdTe)	563	472	410	256
Gaussian width (kHz)	4.9	16.6	4.6	8.4
Assignment	$\text{Te}_3$	$\text{Te}_4$	$\text{Te}_2$	$\text{Te}_1$
Integrated intensity	0.42	0.36	0.15	0.07
Statistical probability	0.418	0.370	0.177	0.033

instead, chose to apply the Hg pulses at other times during the cycle (as shown in Fig. 2), generating a partially coupled spectrum with the available signal intensity spread over a narrower spectral window. Where  $\tau_1$  is the spacing between Te  $\pi$  pulses and  $\tau_2$  is the spacing between Hg  $\pi$  pulses, the scaling factor SF, associated with our experiment (assuming short pulses and calculating only to lowest order) is

$$\text{SF} = \frac{\tau_2}{2\tau_1} - 1,$$

where  $\tau_1 \leq \tau_2 \leq 3\tau_1$ . The resulting spectrum, with pulse

spacings chosen so that dipole-dipole couplings are scaled by approximately 0.05, is displayed in Fig. 3(c). It clearly shows that the most-broadened part of the  $\omega_1$  spectrum correlates with a portion of the chemical shift powder pattern where there is no obvious signal maximum, at 475 ppm. The next-broadest  $\omega_1$  line correlates with the chemical shift peak at 563 ppm. The narrowest part of the spectrum in  $\omega_1$  is at the highest-field (lowest-frequency) portion of the powder pattern. It corresponds to Te<sub>2</sub> (and possibly Te<sub>1</sub> or Te<sub>0</sub>) sites. The experiment was repeated with SF  $\approx$  0.25 and resulted in the spectrum of Fig. 4, where the location of the Te<sub>4</sub> and Te<sub>3</sub> sites is again determined (475 and 563 ppm, respectively).

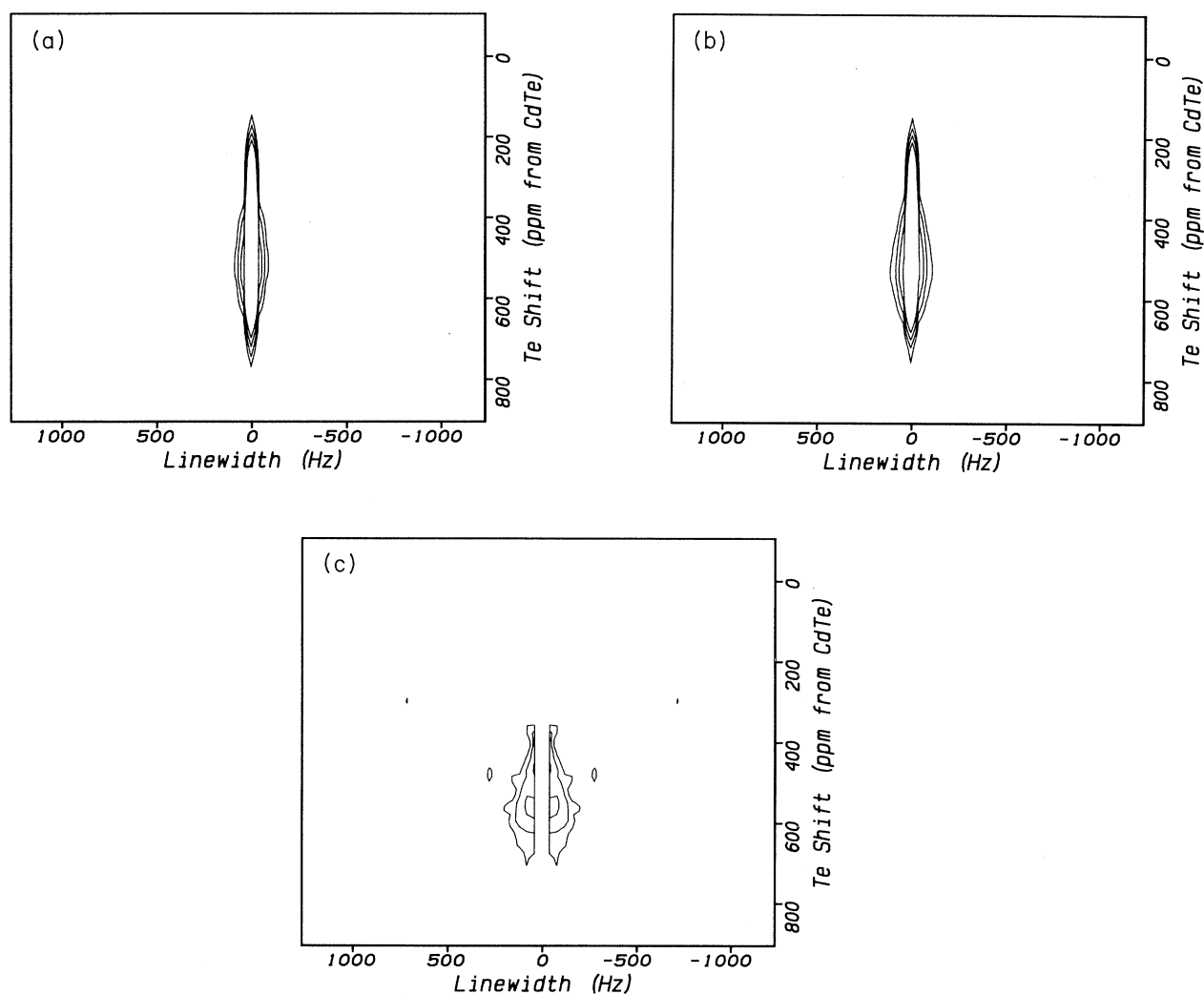


FIG. 3. Dipolar-shift correlation experiments on  $\text{Hg}_{0.78}\text{Cd}_{0.22}\text{Te}$ , based on the experiment of Fig. 2. The  $\omega_1$  dimension represents the Fourier transform associated with time evolution in  $t_1$ , while the  $\omega_2$  dimension represents the Fourier transform of the spin-echo signal starting at its maximum, and is the normal spectrum. The units associated with the  $\omega_1$  dimension are kHz, while those associated with the  $\omega_2$  dimension are Te shifts. (a) Two-dimensional spectrum of all  $^{125}\text{Te}$  sites, with  $^{199}\text{Hg}$  pulses applied in  $t_1$  such that the coupling scaling factor is  $\text{SF} \approx 0.05$ . (b) Two-dimensional spectrum of all  $^{125}\text{Te}$  sites, with no  $^{199}\text{Hg}$  pulses applied in  $t_1$ . The linewidth measured in the  $\omega_1$  dimension is that due to irreversible dephasing and experimental imperfections, only. (c) Difference spectrum, with signal intensity due to  $^{125}\text{Te}$  sites with no  $^{199}\text{Hg}$  neighbors suppressed and contours chosen to reveal correlations. Broadest components (in  $\omega_1$ ) correlate with shifts (in  $\omega_2$ ) at sites with more Hg neighbors.

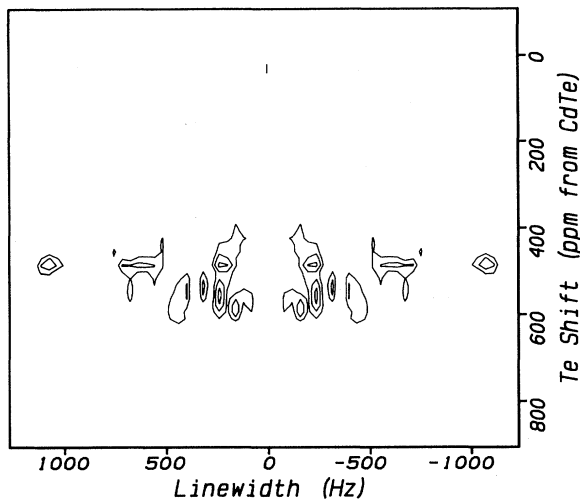


FIG. 4. As in Fig. 3(c), except scaling factor  $SF \approx 0.25$ . The same  $\omega_1$  shifts correspond to the broadest components in  $\omega_2$ .

One hazard inherent in any deconvolution operation is that, given enough adjustable parameters, almost any pattern can be fit to high accuracy. We have managed via two-dimensional NMR to fix several of these parameters, specifically, the band centers for each of the  $Te_3$  and  $Te_4$  environments, the latter shifted by ca. 55 ppm from the spectral band center found in our unconstrained deconvolution, above. Furthermore, an upper bound to the Lorentzian decay constant associated with irreversible dephasing is measured in the Carr-Purcell experiment. This reduces the number of free parameters to a set of line intensities, Gaussian widths (reflecting the distribution of local environments due to inhomogeneities beyond the nearest-neighbor bonds), and line positions for  $Te_2$  and  $Te_1$ . An iterative fit assuming a total of only three lines only poorly reproduces the observed spectrum; a more reasonable fit requiring a total of four lines is demonstrated in Fig. 5. Correlating line positions and identities using Figs. 3(c) and 4, we arrive at the assignments indicated in Table III. Satisfyingly, though the fitting procedure imposed no such condition, these assignments essentially reproduce the bulk composition ( $x = 0.78$ ;  $x_{\text{exp}} = 0.77$ ).

The intensities of the individual microclusters  $P^q(x)$  appear (for this particular melt-grown crystal) to be essentially statistical, i.e.,

$$P^q(x) = \binom{4}{q} x^q (1-x)^{4-q}$$

and therefore in reasonable agreement with available theoretical models for high-temperature grown samples.<sup>2-5</sup> This differs from conclusions drawn previously<sup>7</sup> on poorly characterized powder samples of  $Hg_x Cd_{1-x} Te$ , apparently because (1) the cations in the powder samples appear not to have been distributed homogeneously, (2) the positions of the individual microcluster bands were poorly known, and (3) the  $Te_4$  cluster line proved to be unexpectedly broad.

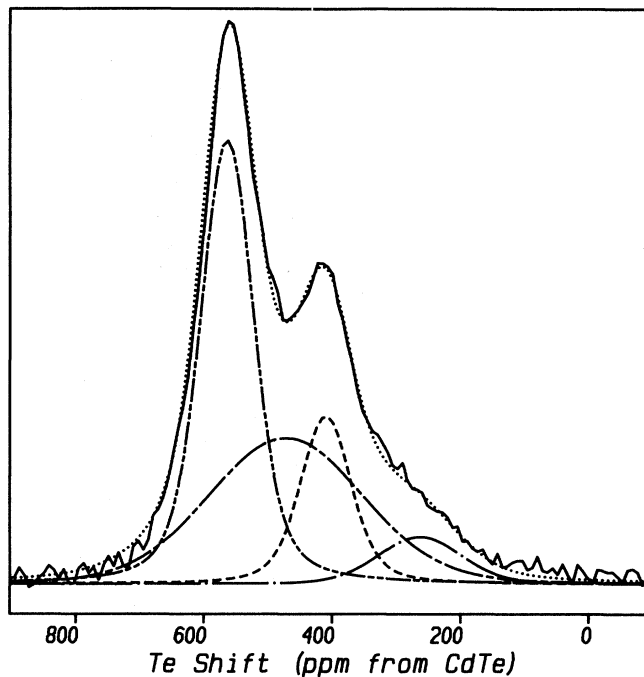


FIG. 5. The experimentally observed spectrum of Fig. 1 for a crystal of  $Hg_{0.78}Cd_{0.22}Te$ , with least-squares fit to spectrum based on four distinct spectral bands, as described in Table II with the band centers derived from the two-dimensional NMR spectra of Figs. 3 and 4. Peak 1, - - - - -; peak 2, - · - · -; peak 3, · · · · ·; peak 4, - · - · -; sum over four subspectra, . . . . .

### Hg NMR

Emboldened by our success in establishing a correlation between chemical environment and NMR spectral frequency, we attempted a simple heteronuclear correlation experiment between Hg and Cd sites (in the second coordination sphere) so as to investigate possible correlations between the observed Hg shifts and their local environment. The first-coordination sphere about any Hg atom is well ordered and consists of four Te atoms; therefore, only the second-coordination sphere (consisting of 12 cations) differentiates between local environments. Should the Hg spectrum consist of a number of overlapping lines corresponding to Hg sites with varying numbers of Cd second-nearest neighbors, we might expect that the Hg-Cd correlation experiment would reveal this correlation. In  $Cd_x Zn_{1-x} Te$  a similar correlation has been shown between Cd shifts and numbers of Zn near neighbors.<sup>24</sup>

Our experiment is a one-dimensional version of the Hg-Te double-resonance experiment described above. It differs, essentially, primarily because the Cd-Hg couplings are significantly smaller and the probability of finding both  $^{199}Hg$  and  $^{111}Cd$  together is relatively small. Thus we are attempting to find a small amplitude change which develops only at fairly long times during which the natural decay in Hg NMR signals was substantial. The resulting low sensitivity made the full two-dimensional

experiment unattractive.

Instead, we measured only a single  $t_1$  time point. Prior to observing the Hg spectrum, a rapid sequence of  $\pi$  pulses were applied on-resonance simultaneously to both  $^{199}\text{Hg}$  and  $^{111}\text{Cd}$ . [As these sites are only second-nearest neighbors in the lattice, the couplings are correspondingly diminished. Furthermore, relatively few  $^{199}\text{Hg}$  have more than a single  $^{111}\text{Cd}$  nearby due to the low concentration of Cd (22% of the cations in the lattice) and the low abundance of the specific isotope we irradiate,  $^{111}\text{Cd}$  (12.75%). Unlike the Hg-Te experiments, there was therefore no need to scale down the coupling amplitude.] The spectrum of the resulting free-induction decay was then compared to that of the same experiment repeated without Cd pulses. The former experiment reflects primarily the spectra of Hg sites *with no* nearby  $^{111}\text{Cd}$  neighbors; the latter reflects the spectra of all Hg sites. The difference spectrum reflects primarily the spectra of Hg sites *with* nearby  $^{111}\text{Cd}$  neighbors.

Under the best of circumstances, we might expect to decrease only partially the  $^{199}\text{Hg}$  signal intensity. A model calculation readily provides the limit to the signal we might destroy. Assume that Cd-Hg couplings are sufficiently large (and our pulse sequence sufficiently efficient) that a signal from any  $^{199}\text{Hg}$  nucleus with even one  $^{111}\text{Cd}$  second-nearest neighbor is eliminated by our pulse sequence. Assume further, for simplicity, that the cations are randomly distributed. Then the maximum signal destroyed is given by the sum

$$\sum_{l=1}^{12} \binom{12}{l} (0.78)^{12-l} (0.22)^l (1 - 0.8725^l) \approx 0.29,$$

where  $l$  is the number of Cd second-nearest neighbors,

$$\binom{12}{l} (0.78)^{12-l} (0.22)^l$$

is the probability of finding  $l$  second-nearest Cd neighbors in a crystal with our overall bulk composition (78% Hg and 22% Cd), and  $(1 - 0.8725^l)$  is the probability that at least one of the  $l$  Cd sites is  $^{111}\text{Cd}$  (and thus irradiated by our Cd pulses). At the opposite extreme, were we to assume that the cations are well ordered and each Hg site has exactly two or three second-nearest-neighbor Cd atoms in the correct proportions for the overall bulk composition, a similar calculation suggests the maximum signal destroyed is 0.30 of the total Hg signal.

Either calculation overestimates our ability to destroy the  $^{199}\text{Hg}$  signal intensity because they ignore the relatively small size of Cd-Hg couplings. Signal intensity is destroyed only if we can preserve Cd-Hg couplings for a time of the order of the inverse of the effective Cd-Hg coupling, and the Hg  $T_2$  is relatively short. Experimentally, the maximum measured intensity difference was 5%. That 5% of the signal lost necessarily came from sites with at least one  $^{111}\text{Cd}$  second-nearest neighbor, and preferentially represents Hg sites with more Cd near neighbors. The spectrum obtained while applying only Hg pulses represents all Hg sites, while the difference between the spectrum obtained with Hg pulses only and the

spectrum with both Hg and Cd pulses represents the spectrum of Hg sites with more Cd neighbors. There was no significant difference observed between the spectrum of Hg sites with at least one  $^{111}\text{Cd}$  second-nearest neighbor and the spectrum of all Hg sites. This suggests that  $^{199}\text{Hg}$  spectral frequencies are determined not by local chemical effects but instead by some nonlocal parameter of longer range. The length scale probed is certainly shorter than the effective range monitored in powder x-ray studies, because it is possible to measure multiple Hg NMR environments in samples with no discernible x-ray splittings due to phase separation. This is in contrast to previous observations based on the Cd NMR spectra in  $\text{Cd}_x\text{Zn}_{1-x}\text{Te}$ , where a clear correlation was established between position in the Cd line shape and the number of Zn neighbors.<sup>24</sup>

No attempt was made to perform similar experiments on the Cd sites. The Cd NMR line position was never observed to be doubled, nor did it shift substantially over the entire range of concentrations observed. Furthermore, excessively long spin-lattice relaxation times  $T_1$  made Cd an unattractive species for particularly demanding experiments. It is somewhat surprising that the magnetic interactions at the Te sites are dominated by local effects, while Hg is dominated by more extended electronic interactions, and the Cd sites are virtual spectators.

This may, however, be a simple reflection of the different participation of the various electronic orbitals.<sup>25</sup> The Knight shifts (which reflect long-range electronic interactions) are primarily due to the overlap of electron orbitals with the nucleus. These interactions are due primarily to  $s$  electronic orbitals. Due to relativistic effects, the Hg  $s$  orbitals overlap strongly with the nucleus. The Cd  $s$  orbitals overlap much less with the nucleus. For Te,  $p$  and  $d$  orbitals contribute more strongly to bonding. These orbitals are relatively inefficient at producing Knight shifts but contribute strongly to chemical shifts. Some aspects of the contributions of the various atomic orbitals to the NMR parameters will be discussed in a separate paper where we will emphasize the dependence of both NMR spectra and relaxation parameters on the electrical properties.

## CONCLUSION

Hg NMR has been shown to monitor long-range electronic environment in  $\text{Hg}_x\text{Cd}_{1-x}\text{Te}$  alloys. In some powder samples where earlier measurements of the Te NMR spectra appeared inconsistent with random distributions of the cations Hg and Cd,<sup>7</sup> subsequent Hg NMR experiments revealing more than one Hg environment suggest that the samples were multiphase. Similar measurements on crystal samples of  $\text{Hg}_{0.78}\text{Cd}_{0.22}\text{Te}$  reveal instead only one Hg environment. With the assistance of a solid-state two-dimensional NMR heteronuclear correlation experiment, we have reevaluated the assignment of Te shifts to chemical environment in a single-crystal sample of  $\text{Hg}_{0.78}\text{Cd}_{0.22}\text{Te}$ . These assignments reconfirm that the Te shift correlates strongly to local (chemical) environment.<sup>7-9</sup> A weaker correlation exists between the Te

shift and bulk properties of the alloy. Hg-Te correlation spectroscopy provides an internally consistent method of assigning a shift frequency to a specific chemical environment, independent of bulk electronic properties. This allows us to analyze more confidently the intensities observed in the  $^{125}\text{Te}$  spectra of a well-characterized, crystalline sample. In these well-characterized alloy samples, the assignments of Te NMR line positions and intensities are consistent with essentially random cation distributions in high-temperature grown melts. Similar conclusions have recently been reached on both bulk and chemical-vapor-deposition (CVD) grown films of  $\text{Ga}_x\text{In}_{1-x}\text{P}$  based on  $^{31}\text{P}$  solid-state NMR measure-

ments.<sup>26</sup> It will be interesting to extend these measurements to other low-temperature grown crystals where there may be some expectation of ordering, but where such ordering is of insufficient range to be observed in diffraction studies.

#### ACKNOWLEDGMENTS

We have greatly benefited from numerous substantive discussions with A. Zunger, and the assistance of M. Went and G. Went in accomplishing the spectral simulations. This work was supported by the Minerva Foundation and by the MRL Program of the National Science Foundation under Grant No. DMR-9121654.

- <sup>1</sup>J. C. Mikkelsen and J. B. Boyce, *Phys. Rev. Lett.* **49**, 1412 (1982); *Phys. Rev. B* **28**, 7130 (1983).
- <sup>2</sup>G. P. Srivastava, J. L. Martins, and A. Zunger, *Phys. Rev. B* **31**, 2561 (1985).
- <sup>3</sup>S. H. Wei and A. Zunger, *J. Vac. Sci. Technol. A* **6**, 2597 (1988); *Phys. Rev. B* **37**, 8958 (1988).
- <sup>4</sup>A. B. Chen, A. Sher, and M. A. Berding, *Phys. Rev. B* **37**, 6285 (1988).
- <sup>5</sup>R. S. Patrick, A. B. Chen, A. Sher, and M. A. Berding, *J. Vac. Sci. Technol. A* **6**, 2643 (1988).
- <sup>6</sup>A. Willig, B. Sapoval, K. Leiber, and C. Verie, *J. Phys. C* **9**, 1981 (1976).
- <sup>7</sup>D. Zax, S. Vega, N. Yellin, and D. Zamir, *Chem. Phys. Lett.* **138**, 105 (1987).
- <sup>8</sup>D. Zamir, K. Beshah, P. Becla, P. A. Wolff, R. G. Griffin, D. Zax, S. Vega, and N. Yellin, *J. Vac. Sci. Technol. A* **6**, 2612 (1988).
- <sup>9</sup>H. M. Vieth, S. Vega, N. Yellin, and D. Zamir, *J. Phys. Chem.* **95**, 1420 (1991).
- <sup>10</sup>W. M. Higgins, G. N. Pultz, R. G. Roy, R. A. Lancaster, and J. L. Schmit, *J. Vac. Sci. Technol. A* **7**, 271 (1989).
- <sup>11</sup>H. R. Vidyantath, *J. Electrochem. Soc.* **128**, 2609 (1981).
- <sup>12</sup>A. Nolle, *Z. Phys. B* **34**, 175 (1979); R. Balz, M. Haller, W. E. Hertler, O. Lutz, A. Nolle, and R. Schafitel, *J. Magn. Reson.* **40**, 9 (1980).
- <sup>13</sup>A. Willig and B. Sapoval, *J. Phys. L* **38**, 57 (1977).
- <sup>14</sup>E. Lippmaa, M. Mägi, A. Samoson, G. Engelhardt, and A.-R. Grimmer, *J. Am. Chem. Soc.* **102**, 4889 (1980); E. Lippmaa, M. Mägi, A. Samoson, M. Tarmak, and G. Engelhardt, *ibid.* **103**, 4992 (1981).
- <sup>15</sup>J. Klinowski, *Progr. Nucl. Magn. Reson. Spectrosc.* **16**, 237 (1984).
- <sup>16</sup>W. Koch, O. Lutz, and A. Nolle, *Z. Phys. A* **289**, 17 (1978).
- <sup>17</sup>See, for example, C. J. Jameson and J. Mason, in *Multinuclear NMR*, edited by J. Mason (Plenum, New York, 1987), Chap. 3; J. D. Kennedy and W. McFarlane, *ibid.*, Chap. 11.
- <sup>18</sup>H. Y. Carr and E. M. Purcell, *Phys. Rev.* **94**, 630 (1954).
- <sup>19</sup>S. Meiboom and D. Gill, *Rev. Sci. Instrum.* **29**, 688 (1958).
- <sup>20</sup>M. Emshwiller, E. L. Hahn, and D. Kaplan, *Phys. Rev.* **118**, 414 (1960).
- <sup>21</sup>D. V. Lang, J. B. Boyce, D. C. Lo, and C. P. Slichter, *Phys. Rev. Lett.* **29**, 776 (1972).
- <sup>22</sup>C. D. Makowka, C. P. Slichter, and J. H. Sinfelt, *Phys. Rev. Lett.* **49**, 379 (1982); *Phys. Rev. B* **31**, 5663 (1985).
- <sup>23</sup>D. Franke, K. Banks, R. Maxwell, and H. Eckert, *J. Phys. Chem.* **96**, 1906 (1992).
- <sup>24</sup>K. Beshah, D. Zamir, P. Becla, P. A. Wolff, and R. G. Griffin, *Phys. Rev. B* **36**, 6420 (1987).
- <sup>25</sup>A. Zunger (private communication); S.-H. Wei and A. Zunger, *Phys. Rev. B* **43**, 1662 (1991).
- <sup>26</sup>R. Tycko, G. Dabbagh, S. R. Kurtz, and J. P. Goral, *Phys. Rev. B* **45**, 13452 (1992).